ACS APPLIED MATERIALS & INTERFACES

Research Article

www.acsami.org

Covalent Polyisobutylene–Paclitaxel Conjugates for Controlled Release from Potential Vascular Stent Coatings

John F. Trant,[†] Matthew J. McEachran,[†] Inderpreet Sran,[‡] Bethany A. Turowec,[§] John R. de Bruyn,[∥] and Elizabeth R. Gillies*[,†,‡]

[†]Department of Chemistry, University of Western Ontario, 1151 Richmond Street, London N6A 5B7, Canada

[‡]Department of Chemical and Biochemical Engineering, The University of Western Ontario, 1151 Richmond Sreet, London N6A 5B9, Canada

[§]Biomedical Engineering Graduate Program, The University of Western Ontario, 1151 Richmond Street, London N6A 5B9, Canada

[∥]Department of Physics and Astronomy, The University of Western Ontario, 1151 Richmond Street, London N6A 5B7, Canada

Supporting Information

ABSTRACT: The development of covalent polyisobutylene (PIB)–paclitaxel (PTX) conjugates as a potential approach to controlling drug release from vascular stent coatings is described. PIB–PTX materials containing ∼24 and ∼48 wt % PTX, conjugated via ester linkages, were prepared. The PTX release profiles were compared with those of physical mixtures of PTX with carboxylic acid-functionalized PIB and with the triblock copolymer polystyrene-*b*-PIB-*b*-polystyrene (SIBS). Covalent conjugation led to significantly slower drug release. Atomic force microscopy imaging of coatings of the materials suggested that the physical mixtures exhibited multiple domains corresponding to phase separation, whereas the materials in which PTX was covalently conjugated appeared homogeneous. Coatings of the conjugated materials on stainless steel surfaces suffered less surface erosion than the physically mixed materials, remained intact, and adhered well to the surface throughout the thirty-five day study. Tensile testing and rheological studies suggested that the incorporation of PTX into the polymer introduces similar physical changes to the PIB as the incorporation of a glassy polystyrene block does in SIBS. Cytotoxicity assays showed that the coatings did not release toxic levels of PTX or other species into a cell culture medium over a 24 h period, yet the levels of PTX in the materials were sufficient to prevent C2C12 cells from adhering to and proliferating on them. Overall, these results indicate that covalent PIB–PTX conjugates have promise as coatings for vascular stents.

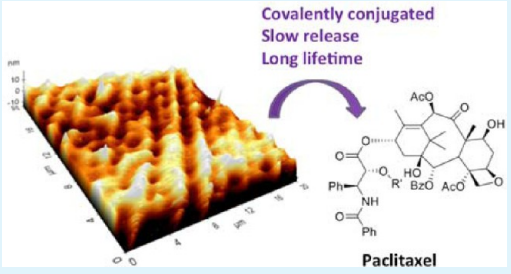

KEYWORDS: *polyisobutylene, butyl rubber, coatings, paclitaxel, arterial stent, SIBS, controlled drug release*

INTRODUCTION

Atherosclerosis is a leading cause of cardiac arrest and is a growing concern for developed and developing societies worldwide.[1] Many treatments are currently available for mild and moderate cases,[2−6] but surgical intervention is often required for more severe cases.[7] To avoid the more invasive bypass surgery, arterial stents can be introduced into an artery to improve blood flow.[8] Early treatments involved bare-metal stents consisting of stainless steel meshes. However, the mechanical damage to tissues resulting from stent implantation results in a cascade of events, ultimately leading to increased cell proliferation and restenosis, the recurrence of arterial blockage.[9] To address this issue, drug-eluting-stents (DES) were developed. These stents release antiproliferative or anti-inflammatory agents that reduce the immune response and vascular smooth muscle cell replication, thereby reducing restenosis.[10,11]

Several types of DES have been developed. The first generation DES are composed of physical mixtures of a drug and a polymer carrier. The Cypher stent uses poly(ethylene-*co*-vinyl acetate) containing sirolimus with a poly(*n*-butyl acrylate) top coating to control drug release, whereas the TAXUS stent uses poly(styrene-*b*-isobutylene-*b*-styrene) (SIBS) containing paclitaxel (PTX).[12,13] Although these stents have been shown to reduce restenosis relative to bare metal stents,[14,15] they still suffer from poor re-endothelialization and the possibility of postimplantation thrombosis. In addition, restenosis is still possible as the drug-release period is sufficient for the initial healing process, but does not necessarily provide long-term protection because of drug depletion.[16,17] An additional disadvantage of these coatings is the possibility of delamination from the stainless steel stent, which would cause a burst release of drug, the release of polymeric coating material into the bloodstream, and the exposure of the bare metal stent, all of which result in significant complications.[18,19] Second generation stents such as Endeavor and Xience employ newer drugs such as zotarolimus and everolimus that are designed to serve as more selective and efficacious antiproliferative agents

Received: May 8, 2015
Accepted: June 11, 2015
Published: June 11, 2015

DOI: 10.1021/acsami.5b04001
ACS Appl. Mater. Interfaces 2015, 7, 14506−14517

for stents.[20−22] Biodegradable polymers such as poly(lactic acid) (PLA) and poly(lactic-*co*-glycolic acid) have also been explored as completely degradable platforms and as stent coatings.[10,11,23−27] The immobilization of heparin as an anticoagulant on the surfaces of stent coatings has been employed with the aim of imparting nonthrombogenic properties, and has been met with variable success.[28−31] The conjugation of antibodies aimed at capturing endothelial progenitor cells to promote re-endothelialization are also being explored.[32,33] Nevertheless, there are limitations to all of these systems and the ideal stent coating has not yet been developed.

Butyl rubber is a copolymer of isobutylene and small amounts of isoprene. The isoprene content provides an alkene functional handle for cross-linking. However, the isoprene units can also be chemically modified to provide a range of functionalities, most commonly through halogenation.[34−36] In previous work, our group reported an efficient and clean epoxidation/elimination sequence that produced an allylic alcohol functionalized polyisobutylene (PIB), which in turn was conjugated to amine-terminated poly(ethylene oxide) (PEO) to provide graft copolymers.[37,38] We have also recently developed carboxylic-acid-functionalized PIBs by reacting the allylic alcohols with cyclic anhydride derivatives.[39] The pendant carboxylic acid moieties were found to enhance adhesion of the polymer to stainless steel and to modify the rheological and tensile properties of the materials.[39] In the current work, we use these pendant carboxylic acid groups as sites for further covalent functionalization to impart new functions to PIB.

As described above, PIB is the main component of the thermoplastic elastomer SIBS,[40−42] which is used in combination with PTX as the coating material on the clinical TAXUS stent.[43,44] PTX is widely used in anticancer treatment, but because of its potent antimitotic activity,[45,46] it is also an excellent antiproliferative for use with cardiovascular stents.[47] Various modifications to SIBS have been explored with the aim of modulating polymer properties and tuning the PTX release rate. For example, arborescent versions of SIBS have been developed and PTX has been physically incorporated.[48] Alternatively, the polystyrene blocks in SIBS have been replaced with polyhydroxystyrene,[49] polyacetoxystyrene,[49] poly(methyl methacrylate),[50] and poly(hydroxyethyl methacrylate).[50,51] Very recently, a PIB−PLA block copolymer with PTX covalently conjugated to the PLA terminus was also reported.[52] However, these systems have resulted in a more rapid release of PTX compared with the original SIBS system, due to the increased hydrophilicity or degradability of the materials. Here we report the application of carboxylic acid-functionalized PIB[39] for the covalent immobilization of PTX at high PTX contents of ∼24 and 48 wt %. We describe the preparation, chemical and physical characterization, and drug release rates from coatings of these materials relative to control systems including SIBS. These release rates are rationalized in relation to the physical properties of the materials and imaging studies of the films before and after 35 days of PTX release. The tensile and rheological properties of these new conjugates are also described, revealing that the conjugation of PTX enhances these properties for their application in stent coatings. A preliminary biological evaluation of the PIB−PTX conjugates is also described.

EXPERIMENTAL SECTION

General Materials and Procedures. Carboxylic-acid-functionalized PIBs **1a** and **1b** were prepared as previously reported[39] from butyl rubber containing 2 mol % isoprene (weight-average molecular weight (M_w) = 340 kg/mol, polydispersity index ($Đ$) = 2.5), and 7 mol % isoprene (M_w = 320 kg/mol, $Đ$ = 2.8) provided by LANXESS Inc. (London, Canada). Solvents were purchased from Caledon Labs (Caledon, Ontario) and all other chemicals were purchased from either Sigma-Aldrich or Alfa Aesar and were used as received unless otherwise noted. SIBS copolymers were obtained from Kaneka (Pasadena, Texas) and donated by LANXESS Inc. Dry toluene was obtained from an Innovative Technology (Newburyport, USA) solvent purification system based on aluminum oxide columns. Dichloromethane and *N*,*N*-diisopropylethylamine (DIPEA) were freshly distilled from CaH_2 prior to use. ^{1}H NMR spectra were obtained in $CDCl_3$ at 400 or 600 MHz on Varian Inova instruments. NMR chemical shifts (δ) are reported in ppm and are calibrated against residual solvent signals of $CHCl_3$ (δ 7.26). Infrared spectra were obtained as films on NaCl plates using a Bruker Tensor 27 instrument. Size exclusion chromatography (SEC) was performed in tetrahydrofuran (THF) with a flow rate of 1 mL/min at 25 °C using an SEC instrument equipped with a Viscotek Max VE2001 solvent module and a Viscotek VE3580 RI detector operating at 30 °C. The stationary phase employed two PolyPore columns (300 mm × 7.5 mm, Agilent) connected in series, equipped with a PolyPore guard column (50 mm × 7.5 mm). Calibration was performed using polystyrene standards. Differential scanning calorimetry (DSC) and thermogravimetric analysis (TGA) were performed on a Mettler Toledo DSC 822e at a heating rate of 10 °C/min. DSC was performed between −100 and +150 °C. Glass transition temperatures (T_g) were obtained from the second heating cycle.

Synthesis of PIBa-cov. An anhydrous sample (dried under vacuum in the presence of P_2O_5) of carboxylic-acid-functionalized PIB **1a** (10 g, 3.9 mmol of CO_2H, derived from PIB containing 2 mol % isoprene),[39] was cut into small pieces and dissolved over 36 h, with stirring, in anhydrous toluene (400 mL) under a nitrogen atmosphere. A solution of 1-ethyl-3-(3-(dimethylamino)propyl) carbodiimide hydrochloride (EDC·HCl, 940 mg, 4.9 mmol), diisopropylethylamine (DIPEA, 1.2 mL, 6.8 mmol), and 4-dimethylaminopyridine (DMAP, 250 mg, 1.95 mmol) were dissolved in anhydrous CH_2Cl_2 (200 mL) and added in one portion to the dissolved polymer. The solution was stirred for 20 min prior to the addition, in one portion, of a solution of PTX (3.7 g, 4.3 mmol) in CH_2Cl_2 (200 mL). The reaction mixture was then stirred at ambient temperature for 16 h. Following NMR determination of conversion, the CH_2Cl_2 was removed under reduced pressure and the toluene solution washed with deionized water, 1 M HCl and twice with 1 M $NaHCO_3$ successively. After reduction of the solution by 2/3 under reduced pressure, precipitation into absolute ethanol provided **2a** as an off-white solid. Yield = 77 %; ∼95 % conversion. ^{1}H NMR (400 MHz, *CDCl*$_3$): δ_{ppm} 8.17 (d, J = 7.4 Hz, 2H), 7.77 (t, J = 7.1 Hz, 2H), 7.62 (t, J = 7.1 Hz, 1H), 7.56−7.45 (m, 3H), 7.44−7.36 (m, 7 H), 7.34 (m, 1H), 7.15−7.10 (m, 1H), 6.30 (s, 1H), 6.29−6.24 (m, 1H), 6.08−6.01 (m, 1H), 5.69 (t, J = 6.1 Hz, 1H), 5.62−5.57 (m, 1H), 5.27−5.19 (m, 1.1H), 5.13−5.06 (m, 1 H), 4.99 (d, J = 9.1 Hz, 1 H), 4.91−4.88 (m, 2H), 4.44−4.40 (m, 1H), 4.37−4.12 (m, 6H), 3.82 (*pseudo*-d, J = 6.5 Hz, 1H), 2.83 (t, J = 6.4 Hz, 1H), 2.62−2.52 (m, 1H), 2.49−2.46 (s, 3H), 2.41−2.35 (m, 1H), 2.26−2.21 (m, 2H), 2.22 (s, 3H) 1.96−1.92 (m, 4H), 1.69 (s, 3H) 1.42 (s, 315H), 1.26−0.91 (m, 950H). IR (thin film on NaCl, chloroform): 1232, 1367, 1390, 1475, 1670, 1737, 2960 cm^{-1}. SEC: M_w = 337 kg/mol, $Đ$ = 1.5. T_g = −62 °C.

Synthesis of PIBb-cov. The conjugate was prepared by the same procedure described above for PIBa-cov, using carboxylic-acid-functionalized PIB **1b** (derived from 7 mol % isoprene, 1.5 g, 1.9 mmol of CO_2H)[39] in 250 mL of anhydrous toluene; EDC·HCl (540 mg, 2.8 mmol), DIPEA (680 μL, 3.9 mmol), and DMAP (110 mg, 0.93 mmol) in 50 mL CH_2Cl_2; PTX (2.0 g, 2.4 mmol) in 100 mL of CH_2Cl_2. Yield = 73%; ∼85% conversion. ^{1}H NMR (400 MHz, *CDCl*$_3$): δ_{ppm} 8.16 (d, J = 7.3 Hz, 2H), 7.74 (d, J = 6.4 Hz, 2H), 7.60

DOI: 10.1021/acsami.5b04001
ACS Appl. Mater. Interfaces 2015, 7, 14506−14517

(t, J = 7.2 Hz, 1H), 7.52 (t, J = 7.6 Hz, 2H), 7.49 (t, J = 7.6 Hz, 1H), 7.44−7.31 (m, 8H), 7.02−6.96 (m, 1H), 6.29 (s, 1H), 6.28−6.20 (m, 1H), 6.08−6.00 (m, 1H), 5.68 (d, J = 6.8 Hz, 1H), 5.62−5.56 (m, 1H), 5.28−5.19 (m, 1.4H), 5.12−5.07 (m, 1.4H), 4.97 (d, J = 9.4 Hz, 1.4H), 4.91−4.89 (m, 1.3H), 4.47−4.41 (m, 1H) 4.40−4.10 (m, 9H), 3.82 (d, J = 6.5 Hz, 1H), 3.70−3.64 (m, 1H), 2.62−2.52 (m, 1H), 2.52−2.44 (m, 4H), 2.42−2.34 (m, 2H), 2.23 (s, 3H), 1.94 (bs, 4H), 1.68 (bs, 3H), 1.41 (s, 112H), 1.29−0.87 (m, 400H). IR: 1232, 1367, 1390, 1475, 1670, 1737, 2960 cm^{-1}. SEC: M_w = 500 kg/mol, $Đ$ = 2.7. T_g = −56 °C.

Preparation of Films. The surface of a stainless steel plate (316L grade steel, with dimensions of 31 mm × 11 mm) was made smooth with a benchtop polisher. The films were prepared from a 100 mg/mL solution of materials in CH_2Cl_2. For the physically mixed samples, PTX was added to achieve the desired weight percentage. A 100 μL aliquot of each of the polymer solutions was drop cast onto the stainless steel plate. The sample was dried under reduced pressure prior to the release study. Each sample was prepared and studied in quadruplicate.

Release Study. The release study was performed in 0.01 M phosphate buffer solution with pH = 7.4, containing 0.138 M NaCl and 0.0027 M KCl and 0.05% (m/v) Tween 20 as a surfactant (Sigma-Aldrich). The stainless steel plates were submerged in 10 mL of buffered solution in a vial. The solution was maintained at 37 °C. The buffer was removed every 7 days for PTX analysis and replaced with fresh medium. Because of the small amounts of PTX released, the release medium was removed via lyophilization and the resulting solid redissolved in 2 mL of 80:20 water:acetonitrile with agitation and filtered through a 2.2 μm syringe filter. A control study demonstrated that PTX was soluble at this concentration.

HPLC Protocol. The HPLC instrument comprised a Waters Separations Module 2695, a Photodiode Array Detector (Waters 2998), and a Nova-Pak C18 4 μm (3.9 mm × 150 mm) column connected to a C_{18} guard column. The PDA detector was used to monitor the PTX absorbance at 228 nm. PTX separation was obtained using a gradient method with Solvent A (5% acetonitrile in water) and Solvent B (80% acetonitrile, 0.1% H_3PO_4 in water) flowing at 1 mL/min. Gradient: Solvent A was decreased from an initial proportion of 65% to 30% over 10 min, and then increased back to 65% over the next 5 min; the column was then allowed to re-equilibrate over 5 min. The calibration curve was obtained from PTX (LC Laboratories, >99%, P-9600) standard solutions. Stock solutions of 1000, 100, and 50 μg/mL PTX in acetonitrile were prepared. The stock solutions were used to make standard solutions of 25, 20, 15, 10, 7.5, 5, 2, 1, and 0.5 μg/mL in 20:80 acetonitrile:PBS solution. Standards were filtered and injected at 100 μL using the above instrument method. Samples were prepared in a 20:80 acetonitrile:PBS solution, filtered through 0.2 μm filters and injected at 100 μL using the same conditions. The limit of detection of PTX was determined to be 0.02 μg. The calibration curve is provided in the Supporting Information.

Atomic Force Microscopy. Surfaces for AFM analysis were those prepared for the release study. Surfaces were visualized using an XE-100 microscope from Park Systems. Images were obtained by scanning the surface at three different resolutions: 20 μm × 20 μm, 5 μm × 5 μm, and 1 μm × 1 μm. Scanning was carried out using rectangular-shaped silicon cantilevers (T300, VISTA probes), with a nominal tip radius of 10 nm and spring constant of 40 N/m. Measurements were performed under atmospheric conditions and at ambient temperature. Topographic (height) and phase (force imaging mode) images were recorded simultaneously in tapping mode. The cantilever was oscillated at its resonance frequency of approximately 300 kHz. All images contained 256 data points per line for 256 lines, and the scan rate was maintained at 1 Hz. Postimaging analysis was carried out using XEI, version 1.7.0 from Park Systems. Images were flattened to remove curvature in both the x and y axes.

Scanning Electron Microscopy. The coated stainless steel plates were mounted on aluminum stubs with carbon tape, then sputter coated with gold. The surface microstructure was then imaged with a S-2600N scanning electron microscope (Hitachi, Japan).

Tensile Testing. Tensile tests were carried out according to ASTM D882-12,[53] using an Instron 3365 universal testing machine. For each sample, 1.5 g of polymer was compressed into 0.3 mm-thick flat sheets using a hydraulic hot press (Carver 3851-0 C). Samples 60 mm × 5 mm in size were cut from this sheet for analysis. The tensile test was performed using a 1 kN load cell and an extension rate of 400 mm/min at ambient temperature (22 ± 1 °C). Load and extension calibrations were preformed prior to the test. To prevent slippage of the samples from the clamps, 10 mm of material was inserted into each clamp giving an effective length of 40 mm. At least six trials were performed for each polymer.

Rheology. Rheological measurements were performed using a TA Instruments AR-1500ex stress-controlled rheometer with a 25 mm-diameter parallel-plate tool. Sandpaper was affixed to both plates to prevent slip. Circular samples 25 mm in diameter and approximately 0.5 mm thick were cut from a sheet prepared by compressing 1.5 g of polymer into a flat sheet using the hydraulic hot press as described above. The sample thickness was measured at three different places. The sample was then placed in the rheometer, the gap between the plates set to the lowest of these measurements, and the sample annealed at 100 °C for 1 h. The sample was then compressed to 90% of the original thickness prior to measurement. Small-angle oscillatory shear measurements were performed at angular frequencies between 0.1 and 100 rad/s with the oscillating stress amplitude controlled at 100 Pa. All rheological measurements were done at 37 °C. The data were averaged over at least four trials for each polymer.

Toxicity Assay. *Sample Preparation.* Test samples were melt-pressed to a thickness of 0.4 mm. The melt-pressed film was then cut into 1 cm × 1 cm squares. Samples were sterilized by washing with 70% ethanol and subsequently dried for 2 h under UV light. They were placed in Petri dishes and incubated in 2 mL of Dulbecco's modified Eagle's medium (DMEM, Invitrogen) supplemented with 10% fetal bovine serum (Invitrogen), 1% Glutamax (100×) solution, and 1% Penstrep (100×) in an incubator at 37 °C for 24 h. The leachate was then removed and passed through a 0.2 μm filter.

MTT Assay. C2C12 mouse myoblast cells were seeded in a Nunclon 96-well U bottom transparent polystyrol plate to obtain approximately 10 000 cells/well in 100 μL of DMEM containing serum, glutamax, and antibiotics as described above. The cells were allowed to adhere to the plate in a 5% CO_2 incubator at 37 °C for 24 h. The growth medium was then aspirated and replaced with either solutions of sodium dodecyl sulfate (SDS) in the cell culture medium at concentrations of 0.2, 0.15, 0.10, or 0.05 mg/mL, which were used as positive controls, serial 2-fold dilutions of the leachate, or fresh medium. The cells were then incubated at 37 °C (5% CO_2) for 24 h. The medium was again aspirated and replaced with 110 μL of fresh medium containing 0.5 mg/mL (3-(4,5-dimethylthiazol-2-yl)-2,5-diphenyltetrazolium bromide) (MTT). After 4 h of incubation (37 °C, 5% CO_2), the MTT solution was carefully aspirated and the purple crystals were dissolved by addition of 50 μL of spectroscopic grade dimethyl sulfoxide (DMSO). After shaking (1 s, 2 mm amp, 654 rpm), the absorbance of the wells at 540 nm was read using an M1000-Pro plate reader (Tecan). The absorbance of wells prepared in the same way but without cells was subtracted as a background and the cell viability was calculated relative to wells containing cells that were exposed only to the culture medium. No (0%) cell viability was detected for cells exposed to the highest concentrations of SDS, confirming the sensitivity of the assay.

Evaluation of Cell Growth on Films. C2C12 cells were maintained at 37 °C and 5% CO_2 in Dulbecco's modified Eagle's medium (Invitrogen) supplemented with 10% fetal bovine serum (Invitrogen) and supplemented with 1% Glutamax (100×) solution and 1% Penstrep (100×). First, microscope glass coverslips (circular, 25 mm diameter) were coated with a minimum layer of polymer by applying a 35 mg/mL (100 μL) solution of polymer in toluene and allowing the solvent to dry completely. The surfaces were sterilized by submersion in 70% ethanol, and were then left to dry completely under reduced pressure for 96 h. The sterilized samples were placed in the wells of a 6-well plate and approximately 5 × 10^5 cells in 2 mL of cell culture medium were seeded onto each surface. The samples were

DOI: 10.1021/acsami.5b04001
ACS Appl. Mater. Interfaces 2015, 7, 14506−14517

Scheme 1. Synthesis of PIB−PTX Conjugates PIBa-cov and PIBb-cov

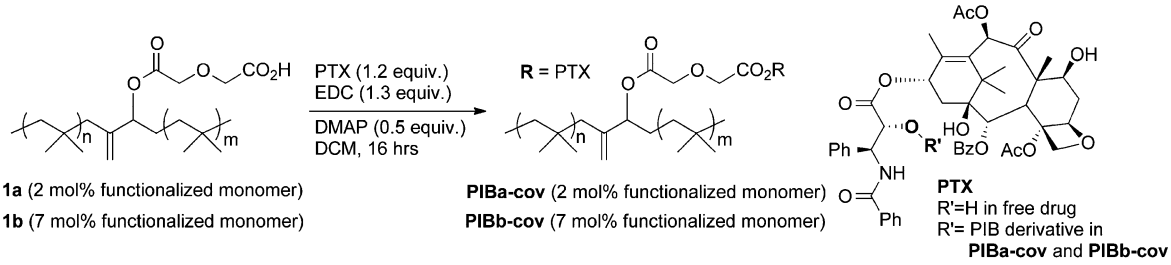

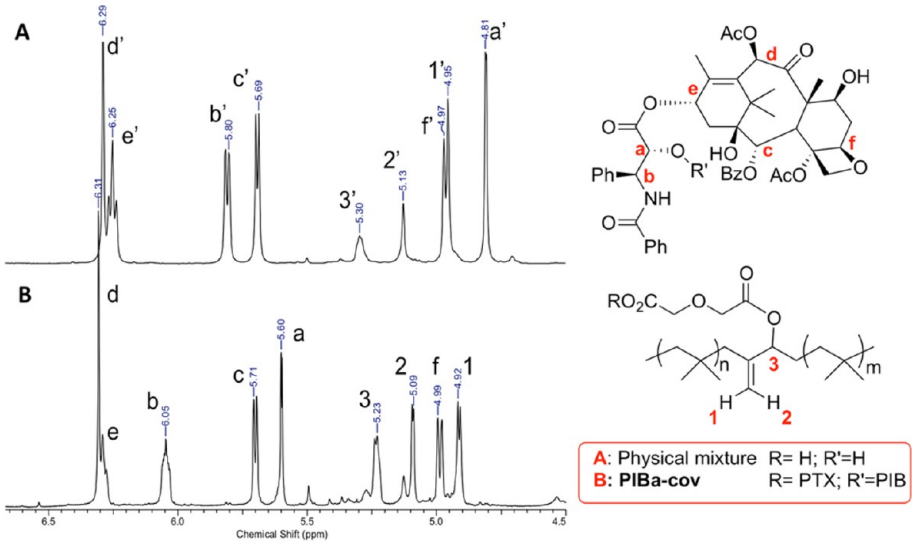

Figure 1. Portion of the ^{1}H NMR spectrum used to determine the success and extent of PTX coupling in PIBb-cov. (A) Physical mixture of PTX and **1a** (′ refers to protons on the uncoupled forms of the polymer and drug). (B) Conjugate PIBb-cov.

incubated for 48 h, then fixed with 4% paraformaldehyde solution for 10 min. The samples were washed twice with phosphate-buffered saline (PBS) (Invitrogen) at pH 7.2, and then treated with 2 mL of acetone at −20 °C for 5 min to permeabilize the membrane. After that, they were washed again with PBS, stained with Alexa Fluor 568 phalloidin (Invitrogen) and DAPI (Invitrogen) following the manufacturer's directions. The samples were washed again with PBS and placed face down onto glass microscope slides with ProLong Gold Antifade Reagent (Invitrogen) and sealed. Confocal images were obtained using a confocal laser scanning microscope (LSM 510 Duo Vario, Zeiss) using a 20× objective and excitation wavelengths of 405 (DAPI) and 578 nm (phalloidin). Cells were counted using Image Pro Plus software on 5 different images. Statistical analysis (ANOVA followed by Tukey's test) was performed using the software Excel and the RealStats add-in.[54]

RESULTS AND DISCUSSION

Synthesis and Characterization of a PIB−PTX Conjugate. The first goal of this work was the development of a simple and rapid synthesis of a covalent PIB−PTX conjugate. To this end, carboxylic-acid-functionalized PIB (Scheme 1) derived from rubber containing either 2 mol % (**1a**) or 7 mol % (**1b**) of carboxylic-acid-functionalized monomer was prepared as recently reported.[39] PTX was then coupled to **1a**/**1b** using 1-ethyl-3-(3-(dimethylamino)propyl)carbodiimide (EDC) in the presence of 4-(dimethylamino)pyridine (DMAP) in CH_2Cl_2 to afford the conjugates PIBa-cov/PIBb-cov. Proton nuclear magnetic resonance (^{1}H NMR) spectroscopy was used to confirm the chemical structures of the conjugates and to estimate the PTX loading. A comparison of the spectra corresponding to a physical mixture of PTX and **1a** (Figure 1a) versus the covalent conjugate PIBa-cov (Figure 1b) confirmed that the drug was conjugated and not physically entrapped. Specifically, an upfield shift of the peak corresponding to the allylic proton of the polymer backbone (labeled 3) from 5.30 to 5.23 ppm was observed upon esterification. This is indicative of reaction near this site. A small amount of residual uncoupled carboxylic acid resulted in the small peak at 5.30 ppm in Figure 1b, but the data indicated that the coupling proceeded in high yield, which is remarkable for the conjugation of a large drug molecule to a polymer backbone.

The peaks corresponding to PTX in Figure 1 were assigned based on previous reports of PTX and PTX 2′ ester conjugates.[55,56] Lataste and co-workers demonstrated that despite the molecule's complexity, esterification of PTX resulted in a single isomeric monoester, as the C2′ hydroxyl group is significantly more nucleophilic than the C7 hydroxyl group.[55] Consequently, a single regioisomeric PTX−PIB conjugate was expected, as indicated in Scheme 1. The large downfield shift of the peak corresponding to the 2′ proton on PTX (labeled a in Figure 1) from 4.81 to 5.60 ppm, and no significant resonance observed at 4.81 ppm suggested that the C2′ hydroxyl indeed underwent esterification in this system. The shift in the peak corresponding to the adjacent benzyl protons (labeled b) from 5.80 to 6.05 ppm was further evidence for this reactivity. The degree of conjugation was quantified by comparing the integrations of the peak corresponding to proton "a" on PTX at 5.60 ppm to the peaks corresponding to the functionalized isoprene units on the polymer backbone (3 and 3′) at 5.30−5.23 ppm [% coupling yield = (integration of

DOI: 10.1021/acsami.5b04001
ACS Appl. Mater. Interfaces 2015, 7, 14506−14517

Table 1. Composition, PTX Loading, and Thickness Measurements of Films Used for the PTX Release Study[a]

sample name	polymer composition	PTX wt %	PTX immobilization	film thickness before release (μm)	film thickness after release (μm)
PIBa-cov	PIBa-cov	~24	covalent	50 ± 10	39 ± 9
PIBb-cov	PIBb-cov	~48	covalent	52 ± 7	67 ± 2
PIBa-phy	**1a**	24	physical	51 ± 4	65 ± 5
PIBb-phy	**1b**	48	physical	25 ± 4	42 ± 9
SIBS1-24	SIBS (15% styrene)	24	physical	58 ± 5	70 ± 4
SIBS2-24	SIBS (30% styrene)	24	physical	60 ± 7	78 ± 2
SIBS1-9	SIBS (15% styrene)	8.8	physical	52 ± 2	65 ± 3
SIBS2-9	SIBS (30% styrene)	8.8	physical	54 ± 4	89 ± 2

[a]Uncertainties correspond to the standard deviation of triplicate measurements.

a/integration of 3 + 3′) × 100]. On the basis of this analysis, the coupling proceeded in ~95% yield for **1a**, affording a PTX content of approximately 24 wt % for PIBa-cov. In the conjugation between **1b** and PTX, the coupling proceeded to ~80% conversion, resulting in approximately 48 wt % PTX for PIBb-cov (Figure S4 of the Supporting Information). On the basis of the M_n values measured by SEC, these correspond to an average of approximately 50 and 112 PTX residues per polymer chain for PIBa-cov and PIBb-cov, respectively.

SEC analysis suggested that there was no significant change in molecular weight for **PIBa-cov**, which had an M_w of 337 kg/mol relative to the starting butyl rubber, which had an M_w of 340 kg/mol when measured relative to polystyrene standards. This suggests that the conjugation of PTX did not have a significant impact on the hydrodynamic volume of the polymer. On the other hand, the M_w of PIBb-cov increased to 500 kg/mol relative to 320 kg/mol for the starting butyl rubber with high isoprene content. The increase in hydrodynamic volume may result from the addition of the 48 wt % of PTX to this system. The compounds were also characterized by TGA and DSC. The TGA traces for both materials showed negligible mass loss below 200 °C, with 5% mass loss at 312 °C for PIBa-cov, and 239 °C for PIBb-cov (Figures S5 and S7 of the Supporting Information). The reported temperature of decomposition for free PTX is approximately 213 °C,[57] whereas those of both the starting 2 and 7 mol % isoprene rubbers as well as their carboxylic acid derivatives **1a** and **1b** are above 300 °C. Thus, the data suggest that while the lower PTX content of PIBa-cov does not significantly impact the thermal stability of the polymer, the stability of PIBb-cov with the higher PTX content approaches that of PTX. DSC suggested that the introduction of even a large quantity of PTX has only a very limited effect on the glass transition point (T_g) of the materials. The T_g of **1a** was previously reported to be −61 °C,[39] and the introduction of 24 wt % PTX in PIBa-cov results in a T_g of −62 °C. Similarly, the T_g of **1b** was reported to be −54 °C,[39] whereas that of PIBb-cov was measured to be −56 °C. Although PTX is known to be a crystalline solid in its pure form with a melting point similar to its degradation temperature, only trace peaks possibly corresponding to melting transitions were observed in the range of 150−200 °C for PIBa-cov and 100−150 °C for PIBb-cov (Figures S6 and S8 of the Supporting Information). However, as the thermal degradation prevented DSC analysis at higher temperatures, the presence of a significant melting transition cannot be excluded.

Preparation of Polymer−PTX Coatings for the PTX Release Study. The drug-release properties of coatings prepared from PIB−PTX conjugates PIBa-cov and PIBb-cov were studied and compared with coatings prepared from several other materials (Table 1). Physical mixtures of PTX and the carboxylic-acid-functionalized rubbers **1a** and **1b** were prepared with the same drug content as in PIBa-cov and PIBb-cov. In addition, samples of SIBS containing 15 and 30 wt % styrene, referred to as SIBS1 and SIBS2 respectively, physically combined with 24 wt % PTX as in the covalent conjugate PIBa-cov or 8.8 wt % PTX as used in a commercial stent coating were also prepared.[58] The coatings were prepared by dissolving the polymer-drug material in toluene at a concentration of 100 mg/mL, filtering the solution, and drop casting 100 μL on 316L stainless steel substrates. The thickness of each coating was measured by AFM prior to the drug release study. As shown in Table 1, most samples had thicknesses of 50−60 μm, with the exception of the mixture of **1b** and PTX, which was considerably thinner. This difference likely results from the very different physical properties of this material, which in turn result from the high carboxylic acid content.[39]

Release of PTX from Polymer−PTX Coatings. The release of PTX from the polymer−PTX coatings was studied according to previously published protocols.[49,59,60] The concentration of released PTX was measured by HPLC every 7 days over a period of 35 days. As shown in Figure 2, all SIBS samples released the drug more rapidly than the PIB-based samples, with the amount of PTX released ranging from 0.4% to 2.5% of total conjugated drug over 35 days for the SIBS

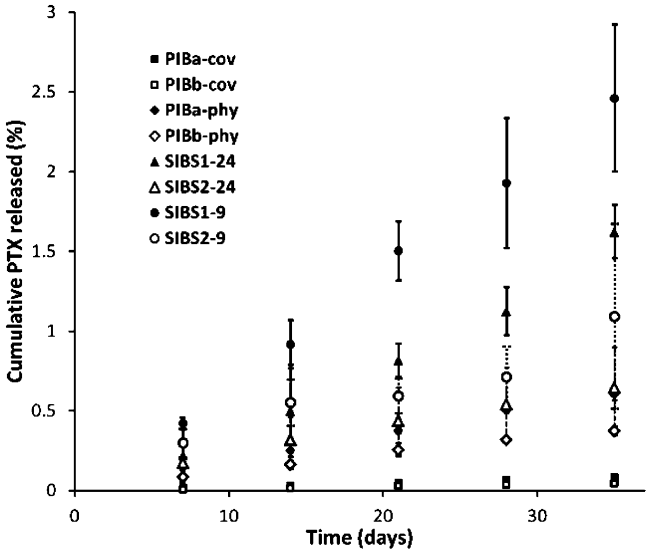

Figure 2. Cumulative percentage of PTX released from the polymeric films listed in Table 1 in aqueous solution at pH 7.4. Data points are the mean of three trials and error bars are standard deviations. Data points for PIBa-cov and PIBb-cov overlap, as do those for SIBS2-24 and PIBa-phy.

DOI: 10.1021/acsami.5b04001
ACS Appl. Mater. Interfaces 2015, 7, 14506−14517

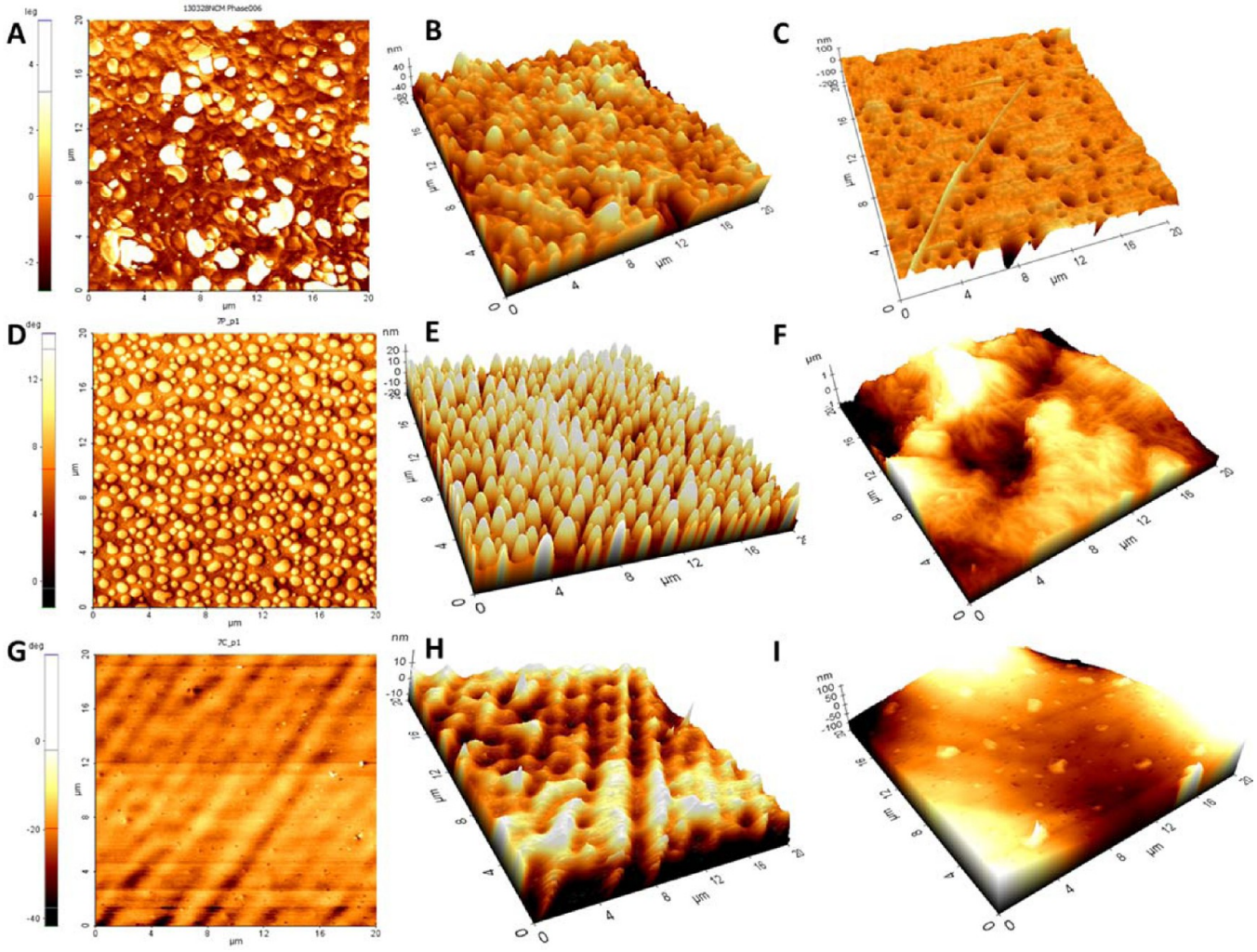

Figure 3. AFM images showing the polymer surface before and after the release study: (A−C) SIBS2-24; (D−F) PIBb-Phy; (G−H) PIBb-cov. Phase images before release: panels A, D, and G. Topography images before PTX release: panels B, E, and H. Topography images after 35 days of PTX release: panels C, F, and I.

materials. SIBS1, which had the lower PS content, released the drug more rapidly than SIBS2, with a higher PS content. The PTX covalently bound to the modified PIB materials was released more slowly than the physically bound PTX, with less than 0.1% of the drug released over 35 days. PIBa-cov and PIBb-cov exhibited the same fractional release rate, although the actual quantity of PTX released was higher for the material with the higher initial PTX loading. PIBb-phy with 7 mol % carboxylic acid released the drug more slowly than PIBa-phy, with 2 mol % carboxylic acid loading in the physically mixed case with ∼0.4% and 0.6% of PTX released respectively over 35 days. Overall, these results suggest that the PIB materials containing covalently bound PTX should exhibit a longer drug-release lifetime than the SIBS materials. In the context of vascular stents, this may provide added protection against restenosis.

AFM Imaging of Films. To gain further insight into the release of PTX from the polymer−PTX films, AFM was used to image the surfaces before and after release. Representative phase and topography images are shown in Figure 3 and additional images are included in the Supporting Information. As depicted in Figure 3a for SIBS2-24, phase images of the SIBS samples containing PTX suggested the presence of different phases within the coatings, and topographical images revealed the presence of irregularly distributed hill-like features 20−30 nm in height and hundreds of nm in diameter on the film surface (Figure 3b). These features were not observed on coatings of SIBS without PTX, when prepared under the same conditions and imaged over the same dimensions (Figures S11−S14 of the Supporting Information). Phase separation and topographical features have been previously reported for SIBS coatings and were proposed to arise from the ability of the rubbery PIB phase surrounding the hard PS to relax and expand out of the surface of the film,[61] but this phenomenon occurred on the low nanometer scale, consistent with the dimensions of the block copolymers.[48,61−63] In agreement with our results, microphase-separated morphologies and similar topographical features have been previously observed on SIBS coatings containing physically incorporated PTX.[64] They have been proposed to correspond to discrete particles of PTX, as no evidence of solubility or molecular miscibility of PTX in SIBS was found by techniques such as DSC or NMR. As shown in Figure 3c, after 35 days of PTX release, the hill-like features had disappeared and were replaced by irregularly distributed valleys. This was also observed in previous studies of SIBS with PTX and likely results from the loss of PTX from the coating

DOI: 10.1021/acsami.5b04001
ACS Appl. Mater. Interfaces 2015, 7, 14506−14517

surface.[64] Similar results were obtained for the other SIBS-based coatings containing PTX (Figure S17−S29 of the Supporting Information).

Phase separation behavior was also observed for the coating comprising a physical mixture carboxylic-acid-functionalized PIB and 48 wt % PTX (PIBb-phy). The phase images of these coatings (Figure 3d) showed two distinct phases that we suggest correspond to the rubber and PTX. Like for SIBS, the topography image (Figure 3e) also revealed a series of hill-like features about, in this case ∼10 nm in height. Following PTX release, a surface of rolling hills was exposed (Figure 3f) that were both higher and much larger in lateral extent. The observed topography may result from the tendency of PIB to shrink during extended exposure to water, especially with loss of PTX from the surface, as well as from the underlying stainless steel substrate (Figure S16 of the Supporting Information). The coating of carboxylic-acid-functionalized PIB and 24 wt % PTX (PIBa-phy) showed less pronouced phase separation and topographical features than PIBb-phy but also underwent a significant topography change following release, to reveal large scale surface features (Figures S30−S34 of the Supporting Information).

The AFM images of films of the covalent PIB−PTX conjugates appeared quite different from those of the physical mixtures. As shown in Figure 3g for PIBb-cov, the phase image suggested that the surface consisted mostly of a single phase, with the apparent texture likely arising from the underlying substrate (Figure S15 of the Supporting Information). This can be explained by the covalent conjugation of PTX to the PIB backbone by the short diglycolic acid linker, which would favor a uniform distribution of the drug throughout the rubber. The topography image (Figure 3h) showed some surface roughness on the order of 2−3 nm, but did not exhibit the distinct hill-like features of the physical mixtures. After PTX release, some large topographical features were observed for PIBb-cov (Figure 3h), which may also arise from the underlying substrate. PIBa-cov also did not exhibit phase separation or topographical features prior to PTX release (Figures S35 and S36 of the Supporting Information), but phase separation and 20−30 nm hill-like features were observed after release (Figures S37 and S38 of the Supporting Information). The origin of these features is unclear at this time.

Representative SEM images of the film surfaces are provided in Figure 4. As shown in Figure 4a,b, the SIBS films suffered considerable surface degradation on the hundred-micrometer scale after 35 days of incubation in aqueous buffer, but no obvious cracks were observed. Although AFM suggested a considerable increase in the micrometer-scale roughness of the PIBa-phy and PIBb-phy films, SEM images showed considerably less damage to the PIBa-phy (Figure 4c−d) than to the SIBS samples. Nonetheless, the images still showed clear fractures in the surface. Images of films of the covalent conjugates (PIBa-cov is shown in Figure 4e,f) looked very similar before and after PTX release, suggesting that film integrity was mostly maintained, unlike any of the physical mixtures.

We also observed partial to complete delamination of the SIBS films from the 316L stainless steel substrate over the 35 day PTX release study (Figure S40 of the Supporting Information). This is likely related, at least in part, to the film damage that was observed by SEM. In contrast, most films prepared from the carboxylic-acid-functionalized PIB did not delaminate. The exception was PIBb-phy, which contained a very high (48 wt %) loading of PTX and partially delaminated. These results suggest that the carboxylic-acid-functionalized PIB materials may have some advantages over SIBS in terms of coating properties. Indeed, we have observed that the carboxylic-acid-functionalized rubbers **1a** and **1b** show enhanced adhesion to stainless steel 316L compared to the parent butyl rubbers,[39] and the covalent PTX conjugates of these materials may retain this advantageous property.

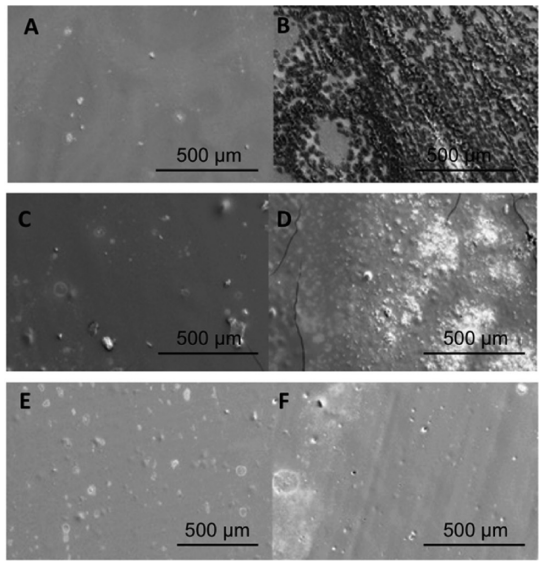

Figure 4. SEM images of polymer−PTX films showing gross structural changes due to the release study. Panels A, C, and E were taken prior to release; panels B, D, and F were taken after release. (A, B) SIBS1-24; (C, D) PIBa-phy; (E, F) PIBa-cov. 100× magnification (except panel C, 95× magnification, and panel E, 80× magnification).

Mechanical and Rheological Properties. The above results suggest that the covalent PIB−PTX conjugates exhibit slow drug release and form smooth, stable films. The mechanical and rheological properties of the materials are also critical to their potential application in vascular stent coatings, as they must survive the process of stent expansion and shear forces due to blood flow. The tensile properties of the new materials were measured and Table 2 provides a comparison of their properties with those of the unfunctionalized butyl rubbers, SIBS1 and SIBS2, as well as the carboxylic-acid-functionalized rubber derivatives **1a** and **1b**.[39] Representative stress−strain curves are shown in Figure 5. Compared to the parent butyl rubbers, as well as the corresponding carboxylic-acid-functionalized derivatives, the PTX conjugates

Table 2. Tensile Properties of the Polymers

material[a]	Young's modulus (MPa)	ultimate tensile strength (MPa)	elongation at break (%)
PIBa-cov	3.7 ± 0.8	3.9 ± 0.6	150 ± 20
PIBb-cov	6.6 ± 0.1	5 ± 2	110 ± 50
SIBS1	2.1 ± 0 0.4	7 ± 2	800 ± 100
SIBS2	3.7 ± 0.4	11 ± 2	530 ± 30
1a	0.35 ± 0.08	1.7 ± 0.3	600 ± 100
1b	3.1 ± 0.8	4 ± 1	140 ± 30
PIBa	0.6 ± 0.1	0.23 ± 0.01	770 ± 70
PIBb	0.59 ± 0.02	0.8 ± 0.2	430 ± 30

[a]Data for **1a**, **1b**, PIBa, and PIBb from McEachran et al.[39]

DOI: 10.1021/acsami.5b04001
ACS Appl. Mater. Interfaces 2015, 7, 14506−14517

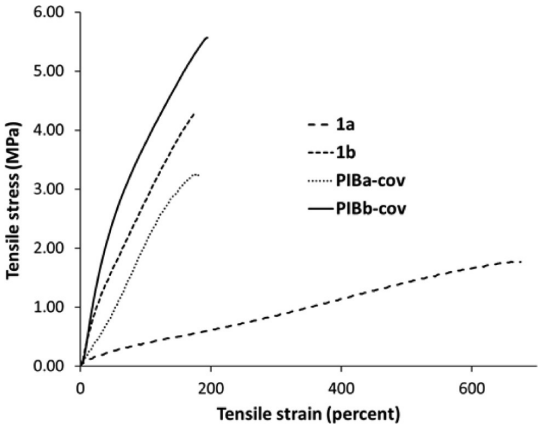

Figure 5. Representative tensile behavior of covalent PTX conjugates and carboxylic-acid-functionalized rubbers. The extension rate was 400 mm/min.

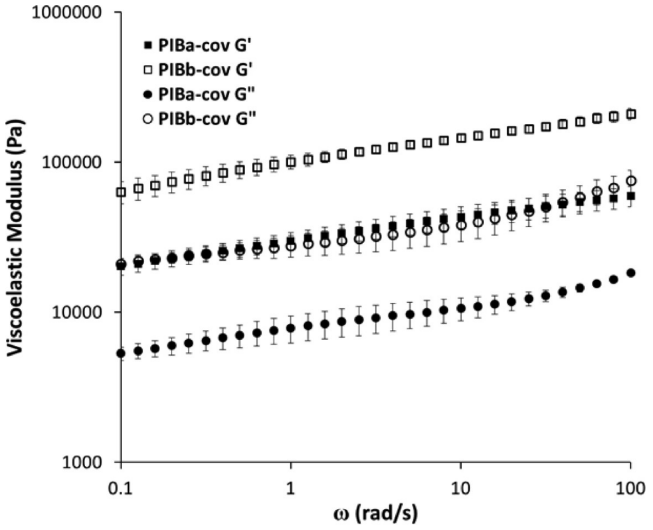

Figure 6. Storage and loss moduli G' and G'' of the PTX conjugates PIBa-cov and PIBb-cov at a stress amplitude of 100 Pa. The data have been averaged over at least three trials, and error bars show the standard deviation.

exhibit greatly increased ultimate tensile strength (UTS) and Young's modulus as well as a corresponding decrease in the maximum elongation, indicative of more brittle elastic behavior. This result might be explained by the formation of nanoscale crystalline domains of PTX. However, as noted above, this crystallinity could not be confirmed in DSC measurements due to the similarity between the T_m for PTX and the decomposition temperature of the polymer. PIBb-cov has a higher Young's modulus and UTS than the PIBa-cov. This trend is similar to what was observed for acid functionalized rubbers **1a** and **1b**, where greater changes in properties relative to the parent rubbers were observed with increased degrees of functionalization.[39] In comparison with SIBS, the strength and modulus of the new conjugates are comparable to those of SIBS1 and SIBS2. However, they are much more brittle, and this limitation should be considered in their optimization and application. This increase in brittleness can likely be attributed to the high PTX content rather the properties of the polymer backbone.[39]

As stent coatings are designed to be used at physiological temperatures, the rheological behavior of the materials was studied at 37 °C. Figure 6 shows the storage and loss moduli, G' and G'' respectively, of the PTX conjugates as a function of frequency ω, measured in small-amplitude oscillatory shear. Both moduli are only weakly dependent on frequency, and for both materials $G' \gg G''$. This behavior is typical of rubber-based materials. The moduli of PIBa-cov and PIBb-cov at $\omega = 1$ rad/s are compared with those of the parent carboxylic-acid-functionalized butyl rubbers[39] and with SIBS in Figure 7. In both cases, the storage and loss moduli of the PIB were substantially increased by the introduction of the PTX, and the material with the higher PTX content had larger moduli than the lower PTX content material. These increases in G' and G'' may arise from the decreased mobilities of the polymer chains upon the introduction of the bulky PTX moieties. A similar effect was recently observed for dynamically cross-linkable PIB gels.[65]

Figure 8 shows tan β, the ratio of the loss modulus to the storage modulus. A value of tan β less than one is indicative of solid-like behavior. The behavior of the PTX-conjugated PIB and the SIBS materials is very similar as tan β is relatively insensitive to frequency at low frequencies, but begins to increase as the frequency rises. This increase in the ratio reflects the slight upturn in G'' that is visible at high ω in Figure 6 and indicates that dissipation due to the motion of the polymer molecules on the scale of the distance between cross-links is becoming important at high frequencies. Similar behavior was observed for other butyl rubber derivatives.[39] These results suggest that the butyl rubber derivatives behave similarly to the SIBS materials in terms of rheology. This is in contrast to the behavior of butyl rubber itself for which tan β does not show a significant frequency dependence.[39] Thus, the introduction of the PTX in a covalent manner imparts rheological properties more suitable to stent applications.

Preliminary Biological Evaluation. The toxicity of the polymers and their effectiveness as antiproliferative coatings is critical to their potential application in vascular stents. The polymers are all insoluble in aqueous solvents, but we investigated the possibility that they could be leaching toxic materials. An MTT assay was performed using various concentrations of polymer leachate to assess cytotoxicity to C2C12 mouse myoblasts, a model cell line. High-density polyethylene (HDPE) was used as a negative control and SDS was used as a positive control (toxicity detected at 0.2 μg/mL, results not shown). According to the ISO standard 10993-5,[66] a cell viability of greater than 70% is indicative of a nontoxic material. The results of the study are shown in Figure 9, and demonstrate that all materials tested are nontoxic by this measure. Importantly, no toxic leachates were detected in any of the PTX-free materials. However, PTX is highly cytotoxic, and the leachates of materials containg PTX did lead to modest reductions in cell viability. These modest reductions in cell viability likely result from the small quantities of PTX released during this assay.

The slow release of PTX from the covalent PIB−PTX conjugates and the lack of toxicity seen in the MTT assay raise the concern that the level of bioactive PTX in the coatings may not be sufficient to impart the desired antiproliferative effects required for DES applications. To investigate this further, the growth of C2C12 cells on the coatings was investigated. Coatings of the polymeric material were seeded with C2C12 cells, incubated for 48 h, then washed to remove cells that had not adhered to the polymer. The cells were fixed and stained with 4′,6-diamidino-2-phenylindole (DAPI, blue, cell nulcei)

DOI: 10.1021/acsami.5b04001
ACS Appl. Mater. Interfaces 2015, 7, 14506−14517

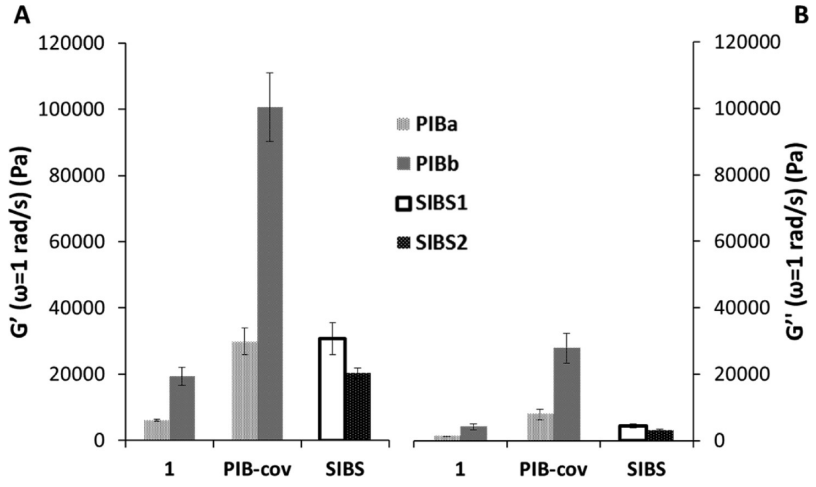

Figure 7. (A) Storage modulus G' and (B) loss modulus G'' of the polymers at ω = 1 rad/s (stress amplitude of 100 Pa), of the carboxylic acid (**1**) and PTX-conjugated (PIB-cov) derivatives of both the low isoprene (PIBa) and high isoprene (PIBb) butyl rubber along with commercial SIBS1 and SIBS2 for comparison. The data have been averaged over at least three trails, and error bars represent standard deviations.

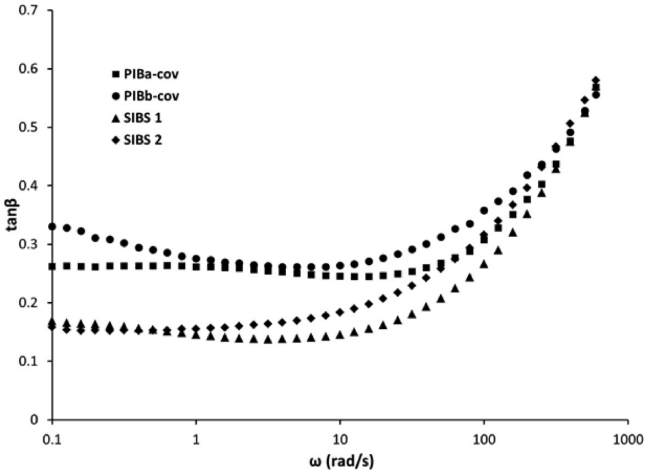

Figure 8. tan β as a function of frequency (stress amplitude of 100 Pa).

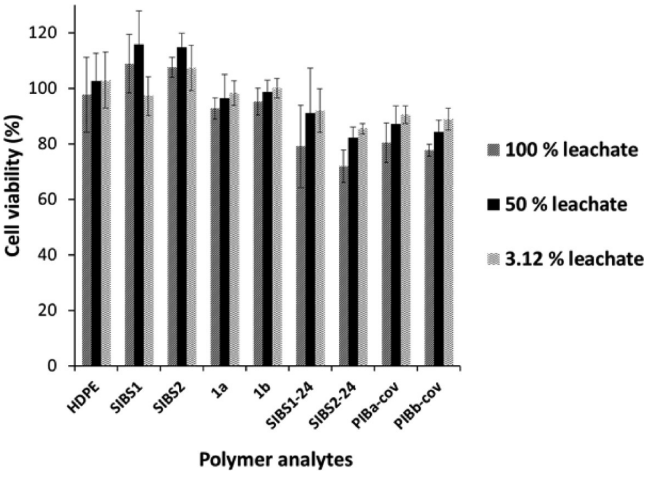

Figure 9. Viability of C2C12 mouse myoblast cells grown in various dilutions of leachate (cell culture medium that was incubated in the presence of polymer materials), as measured by an MTT assay.

and Alexa Fluor 568 phalloidin (cytoskeletons, green), then imaged by fluorescence confocal microscopy. As shown in Figure 10, both butyl rubber (2 mol % isoprene) (Figure 10a) and carboxylic-acid-functionalized rubber **1a** (Figure 10b) were very good substrates for cell growth. The cells appeared healthy, the cytoskeletons normal, and the cells well spread over the polymer surface.

The introduction of PTX resulted in significant changes in cell growth on the surfaces. Most of the PIBa-cov surface was free from cells, although a few cells were able to adhere to isolated regions, as shown in Figure 10c. In these cases, the cells tended to cluster together rather then spread out on the surface, possibly taking advantage of a region of the rubber that had a low PTX content. Most of the surface was free from intact cellular structures and only dead or dying cells and some cellular debris was observed (Figure 10d). On PIBb-cov, which had a higher PTX loading, no clusters of cells were detected (Figure 10e). A few isolated nuclei were observed, but no associated intact cells were observed. These results were quantified by counting the cells adhered to the surfaces. As shown in Figure 10f, there were on average 17 times fewer cells on the low PTX-content PIBa-cov and 65 times fewer on the high PTX-content PIBb-cov than on the surface of **1a**. These results indicate that even though these materials release PTX very slowly, the release rate or the presence of the covelently bound drug is sufficient to prevent cell adhesion and growth on the coatings. This is a promising indicator that these materials may be able to inhibit restenosis in an implanted stent while at the same time minimizing the release of the cytotoxic PTX into the surrounding vasculature, thereby both reducing non-localized toxicity and presumably increasing the lifetime of the stent material.

CONCLUSIONS

We have developed a simple, scalable synthesis of covalent PIB−PTX conjugates. The PTX content of these novel materials was tuned to either 24 or 48 wt % by varying the content of pendant carboxylic acid moieties on the PIB derivatives. The release of PTX from coatings of the PIB−PTX conjugates was studied and compared to that from physical mixtures of PTX with the carboxylic-acid-functionalized PIB and with SIBS. It was found that the release of PTX from the covalent PIB−PTX coatings was significantly slower than from coatings prepared from physical mixtures of PTX and polymer. In addition, AFM imaging suggested that the PTX was likely

DOI: 10.1021/acsami.5b04001
ACS Appl. Mater. Interfaces 2015, 7, 14506−14517

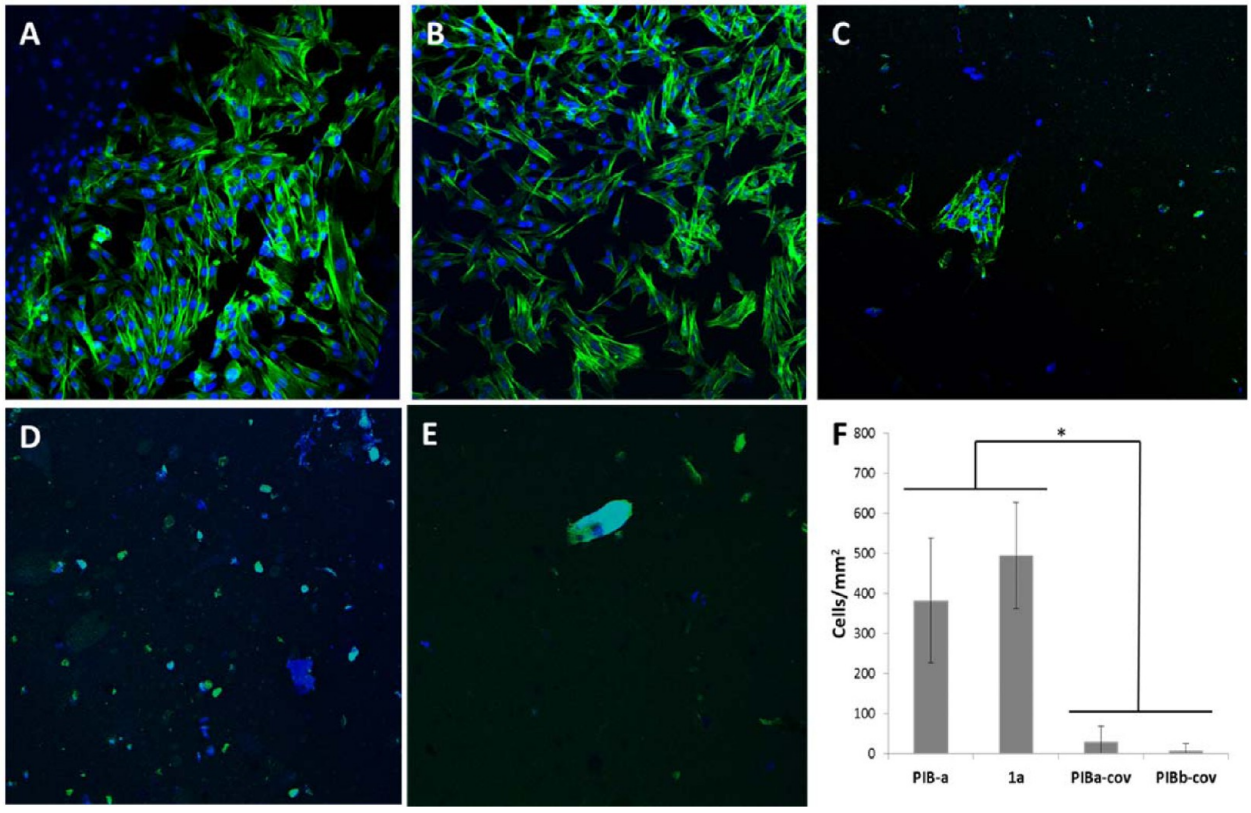

Figure 10. Confocal microscopy images of C2C12 cells on: (A) butyl rubber (2.2% isoprene); (B) **1a**; (C) PIBa-cov, showing a rare region with adherent cells; (D) PIBa-cov, showing a more typical region of the surface; (E) PIBb-cov. (F) Cell counts for the polymers examined (*$P < 0.05$; the two controls are statistically different from the two treatments by ANOVA and Tukey's post hoc test).

distributed evenly throughout the coatings of covalent conjugates, whereas physical mixtures of PTX with carboxylic-acid-functionalized PIB or SIBS displayed phase separation, with the PTX domains likely being eroded during the release study. The introduction of PTX into the polymer matrix changed the tensile and rheological properties of the materials, increasing their elasticity and tensile strength, and making their properties more similar to those of SIBS. An MTT assay revealed that none of the covalent or physically mixed PTX systems released toxic levels of PTX. Despite this, the levels of PTX released or on the surface of the covalently conjugated PIB−PTX coatings were sufficient to prevent the adhesion and growth of C2C12 cells, suggesting that they show the desired antiproliferative effect. Overall, the results of this study demonstrate that covalent PIB−PTX conjugates have promise as vascular stent coatings. Future work will involve further tuning of the biological and mechanical properties of these novel polymers.

■ ASSOCIATED CONTENT

Supporting Information

IR and ^{1}H NMR spectra of the polymers, thermal analysis data, additional AFM images, rheological data, and images showing the delamination of the surfaces over the release period. The Supporting Information is available free of charge on the ACS Publications website at DOI: 10.1021/acsami.5b04001.

■ AUTHOR INFORMATION

Corresponding Author

*E. R. Gillies. E-mail: egillie@uwo.ca.

Notes

The authors declare no competing financial interest.

■ ACKNOWLEDGMENTS

The authors thank LANXESS Inc. and the Natural Sciences and Engineering Research Council of Canada for funding this work, and LANXESS for kindly providing all of the rubber materials. Aneta Borecki is thanked for assistance with the acquisition of the SEC data, Ruiping Ge for assistance with rheology, and Dr. Heng-Yong Nie for assistance with the AFM measurements.

■ REFERENCES

(1) Harris, R. E. *Epidemiology of Chronic Disease: Global Perspectives*; Jones & Bartlett Learning: Burlington, MA, 2013; Chapter 2, pp 25−34.

(2) Libby, P.; Ridker, P. M.; Hansson, G. K. Progress and Challenges in Translating the Biology of Atherosclerosis. *Nature* **2011**, *473*, 317−325.

(3) Moller, D. E.; Kaufman, K. D. Metabolic Syndrome: A Clinical and Molecular Perspective. *Annu. Rev. Med.* **2005**, *56*, 45−62.

(4) Michos, E. D.; Sibley, C. T.; Baer, J. T.; Blaha, M. J.; Blumenthal, R. S. Niacin and Statin Combination Therapy for Atherosclerosis Regression and Prevention of Cardiovascular Disease Events: Reconciling the AIM-HIGH (Atherothrombosis Intervention in Metabolic Syndrome With Low HDL/High Triglycerides: Impact on Global Health Outcomes) Trial With Previous Surrogate Endpoint Trials. *J. Am. Coll. Cardiol.* **2012**, *59*, 2058−2064.

(5) Chyu, K.-Y.; Peter, A.; Shah, P. Progress in HDL-based Therapies for Atherosclerosis. *Curr. Atheroscler. Rep.* **2011**, *13*, 405−412.

(6) Kaliora, A. C.; Dedoussis, G. V. Z.; Schmidt, H. Dietary Antioxidants in Preventing Atherogenesis. *Atherosclerosis* **2006**, *187*, 1−17.

DOI: 10.1021/acsami.5b04001
ACS Appl. Mater. Interfaces 2015, 7, 14506−14517

(7) Al Suwaidi, J.; Berger, P. B.; Holmes, D. R., Jr. Coronary Artery Stents. *J. Am. Med. Assoc.* **2000**, *284*, 1828−1836.
(8) Iqbal, J.; Gunn, J.; Serruys, P. W. Coronary Stents: Historical Development, Current Status and Future Directions. *Br. Med. Bull.* **2013**, *106*, 193−211.
(9) Scott, N. A. Restenosis Following Implantation of Bare Metal Coronary Stents: Pathophysiology and Pathways Involved in the Vascular Response to Injury. *Adv. Drug Delivery Rev.* **2006**, *58*, 358−376.
(10) Khan, W.; Farah, S.; Domb, A. J. Drug Eluting Stents: Developments and Current Status. *J. Controlled Release* **2012**, *161*, 703−712.
(11) Puranik, A. S.; Dawson, E. R.; Peppas, N. A. Recent Advances in Drug Eluting Stents. *Int. J. Pharm.* **2013**, *441*, 665−679.
(12) Fattori, R.; Piva, T. Drug-Eluting Stents in Vascular Intervention. *Lancet* **2003**, *361*, 247−249.
(13) Acharya, G.; Park, K. Mechanisms of Controlled Drug Release from Drug-Eluting Stents. *Adv. Drug Delivery Rev.* **2006**, *58*, 387−401.
(14) Lemos, P. A.; Serruys, P. W.; van Domburg, R. T.; Saia, F.; Arampatzis, C. A.; Hoye, A.; Degertekin, M.; Tanabe, K.; Daemen, J.; Liu, T. K. K.; McFadden, E.; Sianos, G.; Hofma, S. H.; Smits, P. C.; van der Giessen, W. J.; de Feyter, P. J. Unrestricted Utilization of Sirolimus-Eluting Stents Compared With Conventional Bare Stent Implantation in the "Real World": The Rapamycin-Eluting Stent Evaluated at Rotterdam Cardiology Hospital (RESEARCH) Registry. *Circulation* **2004**, *109*, 190−195.
(15) Serruys, P. W.; Kutryk, M. J. B.; Ong, A. T. L. Coronary-Artery Stents. *New Engl. J. Med.* **2006**, *354*, 483−495.
(16) James, S. K.; Stenestrand, U.; Lindbäck, J.; Carlsson, J.; Scherstén, F.; Nilsson, T.; Wallentin, L.; Lagerqvist, B. Long-Term Safety and Efficacy of Drug-Eluting versus Bare-Metal Stents in Sweden. *New Engl. J. Med.* **2009**, *360*, 1933−1945.
(17) Inoue, T.; Node, K. Molecular Basis of Restenosis and Novel Issues of Drug-Eluting Stents. *Circ. J.* **2009**, *73*, 615−621.
(18) Levy, Y.; Mandler, D.; Weinberger, J.; Domb, A. J. Evaluation of Drug-Eluting Stents' Coating Durability—Clinical and Regulatory Implications. *J. Biomed. Mater. Res., Part B* **2009**, *91B*, 441−451.
(19) Ormiston, J. A.; Currie, E.; Webster, M. W. I.; Kay, P.; Ruygrok, P. N.; Stewart, J. T.; Padgett, R. C.; Panther, M. J. Drug-Eluting Stents for Coronary Bifurcations: Insights into the Crush Technique. *Catheter Cardiovasc. Intervention* **2004**, *63*, 332−336.
(20) Carter, A. J.; Brodeur, A.; Collingwood, R.; Ross, S.; Gibson, L.; Wang, C.-A.; Haller, S.; Coleman, L.; Virmani, R. Experimental Efficacy of an Everolimus Eluting Cobalt Chromium Stent. *Catheter Cardiovasc. Intervention* **2006**, *68*, 97−103.
(21) Sketch, M. H., Jr.; Ball, M.; Rutherford, B.; Popma, J. J.; Russell, C.; Kereiakes, D. J. Evaluation of the Medtronic (Driver) Cobalt-Chromium Alloy Coronary Stent System. *Am. J. Cardiol.* **2005**, *95*, 8−12.
(22) Sanchez, O. D.; Yahagi, K.; Koppara, T.; Virmani, R.; Joner, M. The Everolimus-Eluting Xience Stent in Small Vessel Disease: Bench, Clinical, and Pathology View. *Med. Devices (Auckl)* **2015**, *8*, 37−45.
(23) Rossi, F.; Casalini, T.; Raffa, E.; Masi, M.; Perale, G. Bioresorbable Polymer Coated Drug Eluting Stent: A Model Study. *Mol. Pharmaceutics* **2012**, *9*, 1898−1910.
(24) Yang, C.-S.; Wu, H.-C.; Sun, J.-S.; Hsiao, H.-M.; Wang, T.-W. Thermo-Induced Shape-Memory PEG-PCL Copolymer as a Dual-Drug-Eluting Biodegradable Stent. *ACS Appl. Mater. Interfaces* **2013**, *5*, 10985−10994.
(25) Okner, R.; Shaulov, Y.; Tal, N.; Favaro, G.; Domb, A. J.; Mandler, D. Electropolymerized Tricopolymer Based on N-Pyrrole Derivatives as a Primer Coating for Improving the Performance of a Drug-Eluting Stent. *ACS Appl. Mater. Interfaces* **2009**, *1*, 758−767.
(26) Wang, X.; Venkatraman, S. S.; Boey, F. Y. C.; Loo, J. S. C.; Tan, L. P. Controlled Release of Sirolimus from a Multilayered PLGA Stent Matrix. *Biomaterials* **2006**, *27*, 5588−5595.
(27) Raval, A.; Parikh, J.; Engineer, C. Mechanism and in Vitro Release Kinetic Study of Sirolimus from a Biodegradable Polymeric Matrix Coated Cardiovascular Stent. *Ind. Eng. Chem. Res.* **2011**, *50*, 9539−9549.
(28) Hårdhammar, P. A.; van Beusekom, H. M. M.; Emanuelsson, H. U.; Hofma, S. H.; Albertsson, P. A.; Verdouw, P. D.; Boersma, E.; Serruys, P. W.; van der Giessen, W. J. Reduction in Thrombotic Events With Heparin-Coated Palmaz-Schatz Stents in Normal Porcine Coronary Arteries. *Circulation* **1996**, *93*, 423−430.
(29) Vrolix, M. C. M.; Legrand, V. M.; Reiber, J. H. C.; Grollier, G.; Schalij, M. J.; Brunel, P.; Martinez-Elbal, L.; Gomez-Recio, M.; Bär, F. W. H. M.; Bertrand, M. E.; Colombo, A.; Brachman, J. Heparin-Coated Wiktor Stents in Human Coronary Arteries (MENTOR Trial). *Am. J. Cardiol.* **2000**, *86*, 385−389.
(30) Zhao, J.; Falotico, R.; Nguyen, T.; Cheng, Y.; Parker, T.; Davé, V.; Rogers, C.; Riesenfeld, J. A Nonelutable Low-Molecular Weight Heparin Stent Coating for Improved Thromboresistance. *J. Biomed. Mater. Res., Part B* **2012**, *100B*, 1274−1282.
(31) Chen, M.-C.; Chang, Y.; Liu, C.-T.; Lai, W.-Y.; Peng, S.-F.; Hung, Y.-W.; Tsai, H.-W.; Sung, H.-W. The Characteristics and *in vivo* Suppression of Neointimal Formation with Sirolimus-Eluting Polymeric Stents. *Biomaterials* **2009**, *30*, 79−88.
(32) Ako, J.; Bonneau, H. N.; Honda, Y.; Fitzgerald, P. J. Design Criteria for the Ideal Drug-Eluting Stent. *Am. J. Cardiol.* **2007**, *100*, S3−S9.
(33) Li, J.; Li, D.; Gong, F.; Jiang, S.; Yu, H.; An, Y. Anti-CD133 Antibody Immobilized on the Surface of Stents Enhances Endothelialization. *BioMed. Res. Int.* **2014**, *2014*, Article ID: 902782.
(34) Baldwin, F. P. Modifications of Low Functionality Elastomers. *Rubber Chem. Technol.* **1979**, *52*, 77−84.
(35) Jones, G. E.; Tracey, D. S.; Tisler, A. L. In *Rubber Technolology, Compounding and Testing for Performance*; Dick, J. S., Ed.; Hanser: Munich, 2001; pp 178−189.
(36) Malmberg, S. M.; Parent, J. S.; Pratt, D. A.; Whitney, R. A. Isomerization and Elimination Reactions of Brominated Poly(isobutylene-co-isoprene). *Macromolecules* **2010**, *43*, 8456−8461.
(37) Bonduelle, C. V.; Gillies, E. R. Patterning of a Butyl Rubber−Poly(ethylene oxide) Graft Copolymer Revealed by Protein Adsorption. *Macromolecules* **2010**, *43*, 9230−9233.
(38) Bonduelle, C. V.; Karamdoust, S.; Gillies, E. R. Synthesis and Assembly of Butyl Rubber−Poly(ethylene oxide) Graft Copolymers: From Surface Patterning to Resistance to Protein Adsorption. *Macromolecules* **2011**, *44*, 6405−6415.
(39) McEachran, M. J.; Trant, J. F.; Sran, I.; de Bruyn, J. R.; Gillies, E. R. Carboxylic Acid Functionalized Butyl Rubber: Synthesis, Characterization and Physical Properties. *Ind. Eng. Chem. Res.* **2015**, *54*, 4763−4772.
(40) Puskas, J. E.; Chen, Y.; Dahman, Y.; Padavan, D. Polyisobutylene-based Biomaterials. *J. Polym. Sci., Part A: Polym. Chem.* **2004**, *42*, 3091−3109.
(41) Antony, P.; Puskas, J. E.; Kontopoulou, M. Investigation of the Rheological and Mechanical Properties of a Polystyrene-Polyisobutylene-Polystyrene Triblock Copolymer and Its Blends with Polystyrene. *Polym. Eng. Sci.* **2003**, *43*, 243−253.
(42) Puskas, J. E.; Kaszas, G. Polyisobutylene-based Thermoplastic Elastomers: A Review. *Rubber Chem. Technol.* **1996**, *69*, 462−475.
(43) Kamath, K. R.; Barry, J. J.; Miller, K. M. The Taxus Drug-Eluting Stent: A New Paradigm in Controlled Drug Delivery. *Adv. Drug Delivery Rev.* **2006**, *58*, 412−436.
(44) Pinchuk, L.; Wilson, G. J.; Barry, J. J.; Schoephoerster, R. T.; Parel, J.-M.; Kennedy, J. P. Medical Applications of Poly(styrene-block-isobutylene-block-styrene) ("SIBS"). *Biomaterials* **2008**, *29*, 448−460.
(45) Schiff, P. B.; Fant, J.; Horwitz, S. B. Promotion of Microtubule Assembly *in vitro* by Taxol. *Nature* **1979**, *277*, 665−667.
(46) Jordan, M. A.; Wilson, L. Microtubules as a Target for Anticancer Drugs. *Nat. Rev. Cancer* **2004**, *4*, 253−265.
(47) Stone, G. W.; Moses, J. W.; Ellis, S. G.; Schofer, J.; Dawkins, K. D.; Morice, M.-C.; Colombo, A.; Schampaert, E.; Grube, E.; Kirtane, A. J.; Cutlip, D. E.; Fahy, M.; Pocock, S. J.; Mehran, R.; Leon, M. B.

DOI: 10.1021/acsami.5b04001
ACS Appl. Mater. Interfaces 2015, 7, 14506−14517

Safety and Efficacy of Sirolimus- and Paclitaxel-Eluting Coronary Stents. *New Engl. J. Med.* **2007**, *356*, 998−1008.
(48) Puskas, J. E.; Kwon, Y. Biomacromolecular Engineering: Design, Synthesis and Characterization. One-pot Synthesis of Block Copolymers of Arborescent Polyisobutylene and Polystyrene. *Polym. Adv. Technol.* **2006**, *17*, 615−620.
(49) Sipos, L.; Som, A.; Faust, R.; Richard, R.; Schwarz, M.; Ranade, S.; Boden, M.; Chan, K. Controlled Delivery of Paclitaxel from Stent Coatings Using Poly(hydroxystyrene-b-isobutylene-b-hydroxystyrene) and Its Acetylated Derivative. *Biomacromolecules* **2005**, *6*, 2570−2582.
(50) Cho, J. C.; Cheng, G.; Feng, D.; Faust, R.; Richard, R.; Schwarz, M.; Chan, K.; Boden, M. Synthesis, Characterization, Properties, and Drug Release of Poly(alkyl methacrylate-b-isobutylene-b-alkyl methacrylate). *Biomacromolecules* **2006**, *7*, 2997−3007.
(51) Ojha, U.; Feng, D.; Chandekar, A.; Whitten, J. E.; Faust, R. *Langmuir* **2009**, *25*, 6319−6327.
(52) Ren, K.; Zhang, M.; He, J.; Wu, Y.; Ni, P. Preparation of Polymeric Prodrug Paclitaxel-Poly(lactic acid)-b-Polyisobutylene and Its Application in Coatings of a Drug Eluting Stent. *ACS Appl. Mater. Interfaces* **2015**, *7*, 11263−11271.
(53) *Standard Test Method for Tensile Properties of Thin Plastic Sheeting*; ASTM: New York, 2012; D882-12.
(54) Zaiontz, C. *Real Statistics Resource Pack*, Release 3.5. Copyright (2013−2015) www.real-statistics.com.
(55) Lataste, H.; Senilh, V.; Wright, M.; Guénard, D.; Potier, P. Relationships between the Structures of Taxol and Baccatine III Derivatives and their *in vitro* Action on the Disassembly of Mammalian Brain and *Physarum amoebal* Microtubules. *Proc. Natl. Acad. Sci. U. S. A.* **1984**, *81*, 4090−4094.
(56) Deutsch, H. M.; Glinski, J. A.; Hernandez, M.; Haugwitz, R. D.; Narayanan, V. L.; Suffness, M.; Zalkow, L. H. Synthesis of Congeners and Prodrugs. 3. Water-Soluble Prodrugs of Taxol with Potent Antitumor Activity. *J. Med. Chem.* **1989**, *32*, 788−792.
(57) Liggins, R. T.; Hunter, W. L.; Burt, H. M. Solid-State Characterization of Paclitaxel. *J. Pharm. Sci.* **1997**, *86*, 1458−1463.
(58) Boston Scientific Corporation. *Element Stent Series*, 2009.
(59) Strickler, F.; Richard, R.; McFadden, S.; Lindquist, J.; Schwarz, M. C.; Faust, R.; Wilson, G. J.; Boden, M. *In vivo* and *in vitro* Characterization of Poly(styrene-b-isobutylene-b-styrene) Copolymer Stent Coatings for Biostability, Vascular Compatibility and Mechanical Integrity. *J. Biomed. Mater. Res., Part A* **2010**, *92A*, 773−782.
(60) Sirianni, R. W.; Jang, E.-H.; Miller, K. M.; Saltzman, W. M. Parameter Estimation Methodology in a Model of Hydrophobic Drug Release from a Polymer Coating. *J. Controlled Release* **2010**, *142*, 474−482.
(61) Puskas, J. E.; Antony, P.; Kwon, Y.; Kovar, M.; Norton, P. R. Study of the Surface Morphology of Polyisobutylene-based Block Copolymers by Atomic Force Microscopy. *Macromol. Symp.* **2002**, *183*, 191−198.
(62) Puskas, J. E.; Antony, P.; El Fray, M.; Altstädt, V. The Effect of Hard and Soft Segment Composition and Molecular Architecture on the Morphology and Mechanical Properties of Polystyrene−polyisobutylene Thermoplastic Elastomeric Block Copolymers. *Eur. Polym. J.* **2003**, *39*, 2041−2049.
(63) Antony, P.; Kwon, Y.; Puskas, J. E.; Kovar, M.; Norton, P. R. Atomic Force Microscopic Studies of Novel Arborescent Block and Linear Triblock Polystyrene−Polyisobutylene Copolymers. *Eur. Polym. J.* **2004**, *40*, 149−157.
(64) Ranade, S. V.; Miller, K. M.; Richard, R. E.; Chan, A. K.; Allen, M. J.; Helmus, M. N. Physical Characterization of Controlled Release of Paclitaxel from the TAXUS Express2 Drug-Eluting Stent. *J. Biomed. Mater. Res., Part A* **2004**, *71A*, 625−634.
(65) Haldar, U.; Bauri, K.; Li, R.; Faust, R.; De, P. Polyisobutylene-based pH-Responsive Self-Healing Polymeric Gels. *ACS Appl. Mater. Interfaces* **2015**, *7*, 8779−8788.
(66) Tests for *in Vitro* Cytotoxicity. In *Biological Evaluation of Medical Devices*; ISO: Geneva, Switzerland, 2009; 10993-5.

DOI: 10.1021/acsami.5b04001
ACS Appl. Mater. Interfaces 2015, 7, 14506−14517